REGULAR PAPER

Energy Consumption and Tool Condition in Friction Stir Processing of Aluminum Alloys

Alessia Teresa Silvestri[1] · Andrea El Hassanin[1] · Giorgio de Alteriis[2] · Antonello Astarita[1]

Abstract

Friction Stir Welding (FSW) and Friction Stir Processing (FSP) are solid-state joining and material processing techniques that have garnered considerable attention for their versatility and industrial applicability. In the present work, FSP was performed on AA 6056 T4, dealing with the issue of monitoring tool wear and assessing its impact on the process. The impact of tool wear on power requirements was analyzed, and it was expanded the understanding of tool behavior and its implications for the overall process performance. Specifically, variations in energy consumption, temperatures, and vibrations are observed with changing tool conditions. Further insights are provided by analyzing the microhardness and the pin volume ratio, which show distinct trends as the tool wears. Two tool maintenance ways are proposed, that are cleaning the tool with a sodium hydroxide solution and increasing the tool's rotational speed. Both the strategies exhibit the potential to partially restore the tool's initial characteristics. This study highlights the critical importance of assessing tool condition, energy consumption, and process sustainability, particularly in industrial settings where material processing requires efficiency and quality assurance.

1 Introduction

Friction Stir Welding (FSW) has gained a lot of interest as a solid-state joining process due to its intriguing potentialities [1, 2]. Extensive research has been conducted to explore the feasibility of the process for various alloys [3–6] and configurations [7, 8], and fundamental studies, both numerical and experimental, have been carried out to understand the physics of the process and the underlying mechanisms [9–12]. Along with the FSW development, Friction Stir Processing (FSP) has emerged as an interesting process variant. Developed by Mishra et al. in 2000 [13, 14], the aim of FSP is not to join but to refine the microstructure of a given part, following the same steps as in the FSW process. The fundamental principle of FSP is based on the insertion of a rotating pin into a monolithic workpiece, with the shoulder of the tool making contact with the base metals. As the tool moves along its path, the rotation of the shoulder, combined with the applied pressure, generates heat in the surrounding metal. Meanwhile, the rotating action of the pin induces metal from each section to flow and form the processed area [15]. This results in a refined microstructure within the workpiece, offering opportunities for enhancing its properties to suit various applications [16, 17]. As technology becomes more reliable and mature, industrial applications rise up, so new aspects of the process need to be studied: tool wear, energy consumption and sustainability of the process, and monitoring of the process [18–22].

Tool wear is a key factor affecting the part quality, processing efficiency, manufacturing costs, and tool life [23–26]. Therefore, monitoring and considering tool wear during FSP is very important for improving process performance and extending tool lifespan. The wear in FSP has been scarcely studied, while several papers have investigated the wear during FSW [27–30]. However, considering the similarities in tool loads between the two processes, the results obtained for FSW were also considered and discussed in this paper. Previous studies demonstrated that the tool design rules the plastic flow around the tool tip and, in turn, affects the quality of the weld [31]. The shape of the

✉ Alessia Teresa Silvestri
   alessiateresa.silvestri@unina.it

1 Department of Chemical, Materials and Production Engineering, University of Naples "Federico II", P.le Tecchio 80, 80125 Naples, Italy

2 Department of Industrial Engineering, University of Naples "Federico II", P.le Tecchio 80, 80125 Naples, Italy

tool tip influences both temperature development and material mixing along the joint line. Moreover, the tool size has been shown to significantly affect the properties of dissimilar joints, along with variable combinations of the tool speed and feed rate in AA6061 and copper joints [31].

Tool wear is the most significant factor governing tool useful life in FSW and FSP [32], but tool wear monitoring is a major challenge in both processes. Abrasive wear and adhesive wear are two distinct mechanisms identified in prior investigations [33, 34]. The former refers to the abrasion resulting from the displacement of material from a solid surface caused by the sliding of hard particles or protuberances along the surface, while adhesive wear is characterized by the transfer of material during relative motion facilitated by solid-phase welding. In this process, particles removed from one surface adhere permanently or temporarily to the other surface [35]. In addition, the reaction between the tool material and its environment also contributes to tool wear [36]. Severe wear and, consequently, failure predominantly occur in the pin part of the tool, leading to downward material loss and changes in pin geometry. Therefore, in a worn tool, it is possible to observe alterations in the shape of the tool pin [33], which affect process dynamics and part quality [37–39]. However, detecting and monitoring tool wear present substantial challenges. The development of effective monitoring techniques to track the tool condition degradation is important for maintaining high production efficiency and ensuring quality standards. Consequently, the field of joining processes has gradually directed attention towards tool condition monitoring [39], considering that numerous defects in welds can also be attributed to poor tool conditions. Monitoring the condition of the tool enables the prediction of its behavior during the welding process [40]. With usage, every tool undergoes gradual or progressive wear after a certain welding duration. Unusual tool conditions give rise to vibrations, noise, and other detrimental effects that can damage the workpiece [41]. Hence, the analysis of tool condition becomes crucial. Vibration-based analysis stands out as one of the most effective non-destructive methods, enabling the identification of specific elements values and facilitating the assessment of component health [42, 43]. Although some authors have characterized tool wear by tracking material loss along a length of weld, no reliable methodology for monitoring and assessing tool wear during the process has been established [32, 35]. The most common method for monitoring and evaluating tool wear is a direct offline measurement, which often overlooks the intricate physics of the welding process [33].

Despite these studies, a reliable methodology for monitoring and assessing tool wear during the process has not yet been released. Furthermore, studies regarding energy consumption during the process are even more scarce. Considering that tool wear directly affects the properties of the welded or treated parts, it can be argued that it also affects energy consumption. In the context of friction stir processing of aluminum alloys, the abrasive wear of the tool can be neglected, and the tool is considered non-consumable [44–47]. However, the adhesion of material on the tool tip is a commonly observed phenomenon; this adhered material changes the tool geometry and behaves as a built-up edge (BUE) encountered in machining processes. The formation of this BUE could result in increased energy consumption and vibrations.

This paper aims to address the aforementioned challenges by proposing an effective methodology for monitoring and assessing the tool conditions during the service and in studying the energy consumption to assess the sustainability of the process. By analyzing temperature, energy consumption, and vibrations as monitored outputs, this research aims to develop a comprehensive understanding of tool wear and its impact on process performance.

2 Experimental

Aluminum sheets of AA 6056 T4 were utilized as the workpiece for FSP, whose detailed chemical composition and mechanical properties are fully available in literature and not reported here for the sake of brevity [48, 49]. The sheets were rectangular with 200 mm length, 100 mm width and 6 mm thickness. The tool employed in the experiments was provided by FPT Industries and was made of H13 steel. As depicted in Fig. 1, it consisted of a three flat threaded tool with a shoulder diameter of 13 mm, a pin length of 3.15 mm, and a pin diameter of 1.4 mm.

A milling machine ADRIA Machine FEL-660HG, equipped with a customized clamping system, was used to perform the FSP experiments.

To facilitate understanding of the experimental campaign, Fig. 2 presents the flow-chart of the proposed monitoring system. The power consumption of the FSP machine was measured to assess the full machine power during the process as the tool conditions vary. Furthermore, the vibrations induced on the tool were assessed, and the temperature was measured at eight points near the tracks.

The monitoring system is composed of several sensors, described in detail below. A Montronix PulseNG accelerometer was used to acquire the vibrations during the process; the accelerometer was mounted on the spindle head to measure the vibrations acting on the tool. The accelerometer was based on Micro-Electro Mechanical Sensors (MEMS) technology, and the technical specifications are reported in Table 1.

The temperature was measured by using type K thermocouples and a RS 200 Pro data logger. The thermocouples were inserted into 2 mm deep holes drilled on the top surface

**Fig. 1** Shape of the tool used in this experimentation: **a**) top view and **b**) side view
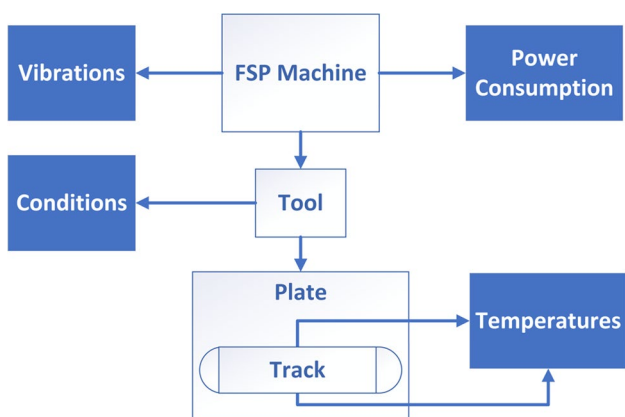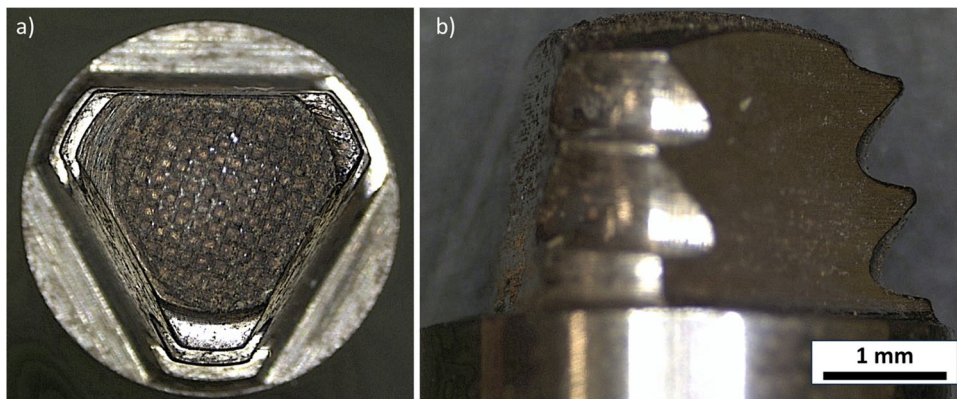
Fig. 2 Flow-chart of the proposed monitoring system for FSP

Table 1 PulseNG accelerometer technical specification

PulseNG Accelerometer	
Measurement Range	$\pm 60\ m/s^2$
Output Linearity	0.1% *F.S.*
Bandwidth	1.6 *kHz*
Resolution($\pm 2g / \pm 6g$)	0.01 m/s^2 /0.03 m/s^2

Fig. 3 Thermocouples and processed tracks position on the sheets
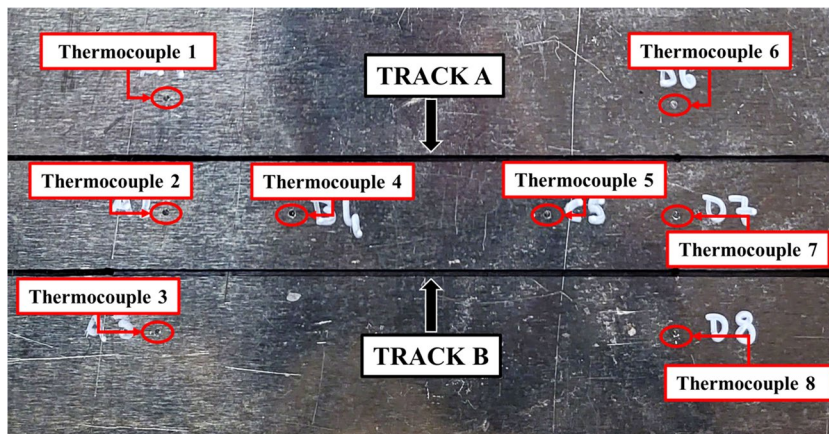
of the plates. In total, eight thermocouples were strategically positioned to map the temperature distribution within the workpiece during the process. A scheme of the thermocouples is given in Fig. 3. As shown in the same figure, two processed tracks were produced on each sheet (tracks to be processed were highlighted with black markers on the sheets). In order to monitor temperature variations, four thermocouples were placed in the middle of the sheets to record the temperature for both Track A and Track B. Additionally, two thermocouples were positioned at the external regions of the sheets to monitor the initiation and completion stages of the process, for both track A and B. This arrangement allowed for comprehensive temperature data collection across different locations within the sheets throughout the entire process.

Power consumption was measured during all the processing operations by means of a power monitoring device, i.e., the Qualistar Plus Power and Energy Quality Analyser CA8331. It is equipped with three current sensors, the Rogowski coils MiniFLEX MA 193–350, four tension cables and four crocodile clips [50]. The milling machine utilized a three-phase connection without a neutral line, with current and voltage values of 32 A and 380 V, respectively. Consequently, data acquisition was carried out by means

of three crocodile clips for the voltage measurements, and three Rogowski coils for the current measurements, with a sampling period of one second. Figure 4 illustrates the full experimental setup, highlighting: *i)* the accelerometer placed on the FSW motor (highlighted in the orange box); *ii)* the thermocouples installed on the plate (highlighted in the red circles); and *iii)* the power analyzer that is mounted between the power source and the FSW machine (highlighted in blue boxes). Figure 5a shows the energy monitoring set-up in detail, including the connections of the voltage probes and Rogowski coils, as illustrated in the schematic representation in Fig. 5b.

The experimental campaign was conceived to monitor the process under various process conditions, which can be divided in four main groups, as follows:

i)   New tool;
ii)   Used tool;

iii) Used tool but cleaned with a sodium hydroxide solution;
iv)   Used tool but increased rotational speed.

The last two groups were designed with the aim to regenerate the tool in an economical manner; group iii) involves a quick and cost-effective removal of the adhered aluminum from the tool tip surface, while group iv) consists in trying to promote a better material flow by increasing the tool rotational speed (TRS) and the linked heat input. This condition is particularly interesting because, although increasing the rotational speed leads to higher power consumption, it may also facilitate improved material flow and greater material softening, potentially reducing the required energy.

Regarding the cleaning procedure, a sodium hydroxide solution was prepared by dissolving 10 g of sodium hydroxide pellets in 90 g of distilled water. The tool was subsequently immersed in the beaker containing the sodium

Fig. 4 Experimental setup: **a**) FSP system with the accelerometer, **b**) power analyzer, **c**) thermocouples
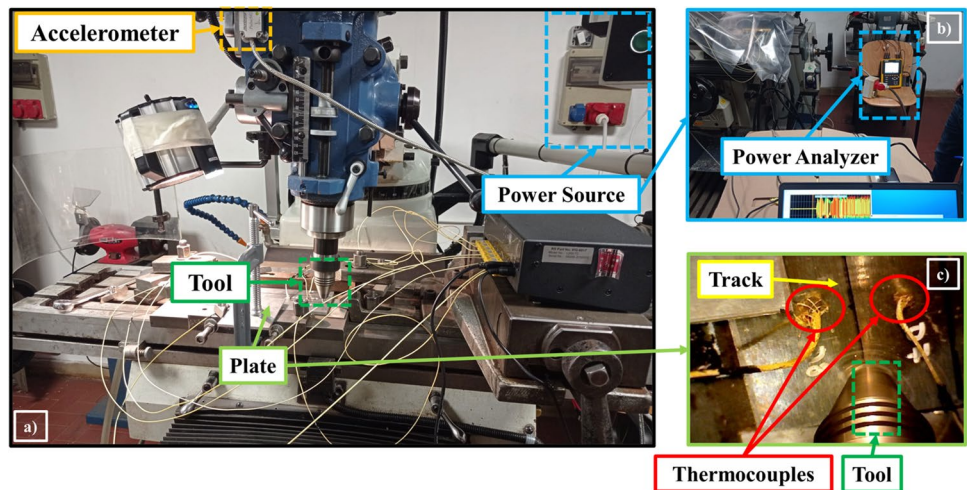
Fig. 5 Energy monitoring setup: **a**) power analyzer connections with the power source cables, **b**) connection scheme
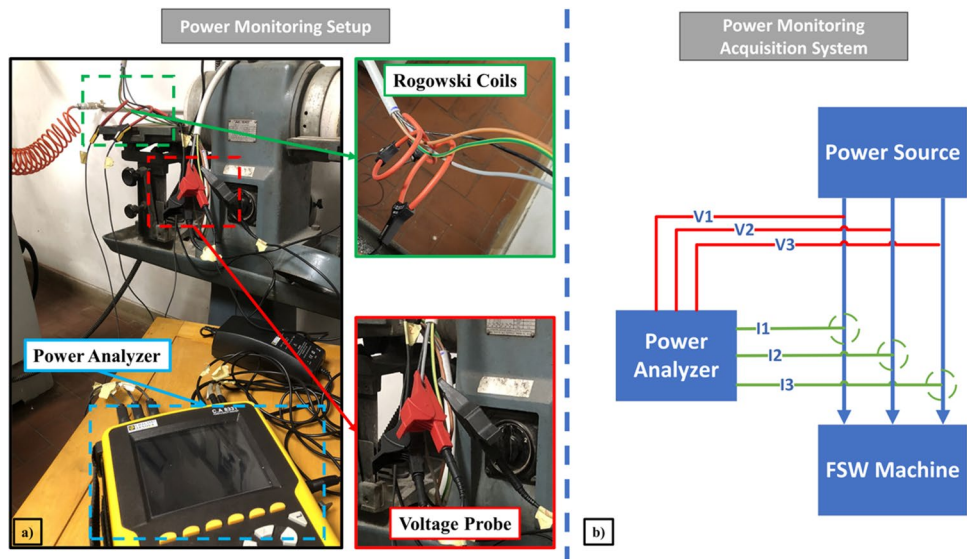
hydroxide solution and placed in an ultrasonic bath for 2 h, at room temperature.

Group ii), iii) and iv) each include two conditions: "Used Tool" (hereinafter indicated as UT), and "More Used Tool" (hereinafter indicated as MUT). The discriminant is the number of times the tool was used between one condition and the other, which is equal to 5.

The experiments consisted in producing treated straight FSP tracks, with a fixed length of 180 mm. A summary of the monitored experiments and corresponding samples (tracks) is provided in Table 2. However, as previously mentioned, it is important to highlight that the total number of FSP tracks performed exceeds those listed in Table 2, specifically, seven conditions, considered more representative, were monitored. Table 2 also summarizes the codes used, which consider the tool condition and the proposed tool maintenance procedure.

In the first monitored experiment, an FSP track was produced with a completely unused tool, therefore the tool condition was indicated as "New Tool" (NT). In experiment 2, the tool condition was denoted as "Used" because, between the two tracks, the tool underwent five further usages. This ensured the measurement and monitoring of a tool in a "used" state, and also for sample 3, i.e. MUT.

In Samples 4 and 5, the tool was thoroughly cleaned, hereinafter indicated as C-UT and C-MUT, respectively, while in Samples 6 and 7, the rotational speed was increased to 2500 rpm, hereinafter indicated as IS-UT and IS-MUT, respectively.

Beyond the NT condition (Fig. 1), the tool in each investigated condition is shown in Fig. 6.

It is important to emphasize that the additional FSP tracks were performed to ensure a comprehensive evaluation of the tool's performance and its response to various conditions.

The quality of FSP was also investigated through Vickers microhardness measurements and microstructure analysis, both conducted on the cross-section of the processed tracks, and macrographic observations were also performed to complete the analysis.

Specimens for microhardness measurements and macrographic observations were prepared by cutting sections from the processed sheets by means of a metallographic cutter. These sections were then hot-mounted in epoxy resin and polished until the surface finish was 1 μm. Optical macrographs were collected using a Zeiss Axioskop 40 instrument, while Vickers microhardness measurements were performed using a Rupac CSV microindenter with a 100 g load and a dwell time of 15 s. Each treated track was subjected to 21 indentations. Specifically, for each specimen, three rows of indentations were made, with each row consisting of 7 indentations. The first row was positioned at 1.5 mm from the upper surface, and the distance between rows was 1.5 mm, the distance between two consecutive indentations of the same row was 2 mm. A schematic representation of the indentation strategy is given in Fig. 7.

3 Results

Images of the top view of the FSP tracks are given in Fig. 8.

Looking at Fig. 8, it is possible to appreciate that all the treated tracks appear free from superficial defects, such as grooves or cracks [17]. Furthermore, the width of the tracks is also quite regular, indicating effective processing and adequate tool-to-sheet contact [2]. As a difference among the different tracks, it can be noted that the amount of flash produced varies and, in particular, increases with the increase of the tool wear.

As mentioned in the previous section, the power required to perform the treatment was continuously measured and recorded through the Qualistar Plus Power and Energy Quality Analyser CA8331. A plot relative to the NT sample (see Table 2), but representative of all the experiments, is displayed in Fig. 9.

From the acquired data, it is possible to distinguish the three different stages of the process, as described by [51, 52], and in particular: I) plunging phase: the tool is rotating at the desired TRS and it is slowly plunged within the plate to be

Table 2 Summary of the experimental campaign and codes used

Sample	Tool Condition	No. of usages	Code	TRS [rpm]	Travel Speed [mm/min]	Plunging depth [mm]	Tilt angle [deg]
1	New	0	NT	2000	40	2.9	2
2	Used	5	UT	2000	40	2.9	2
3	More Used	10	MUT	2000	40	2.9	2
4	Cleaned-Used Tool	15	C-UT	2000	40	2.9	2
5	Cleaned-More Used Tool	20	C-MUT	2000	40	2.9	2
6	Increased Speed-Used Tool	25	IS-UT	2500	40	2.9	2
7	Increased Speed-More Used Tool	30	IS-MUT	2500	40	2.9	2
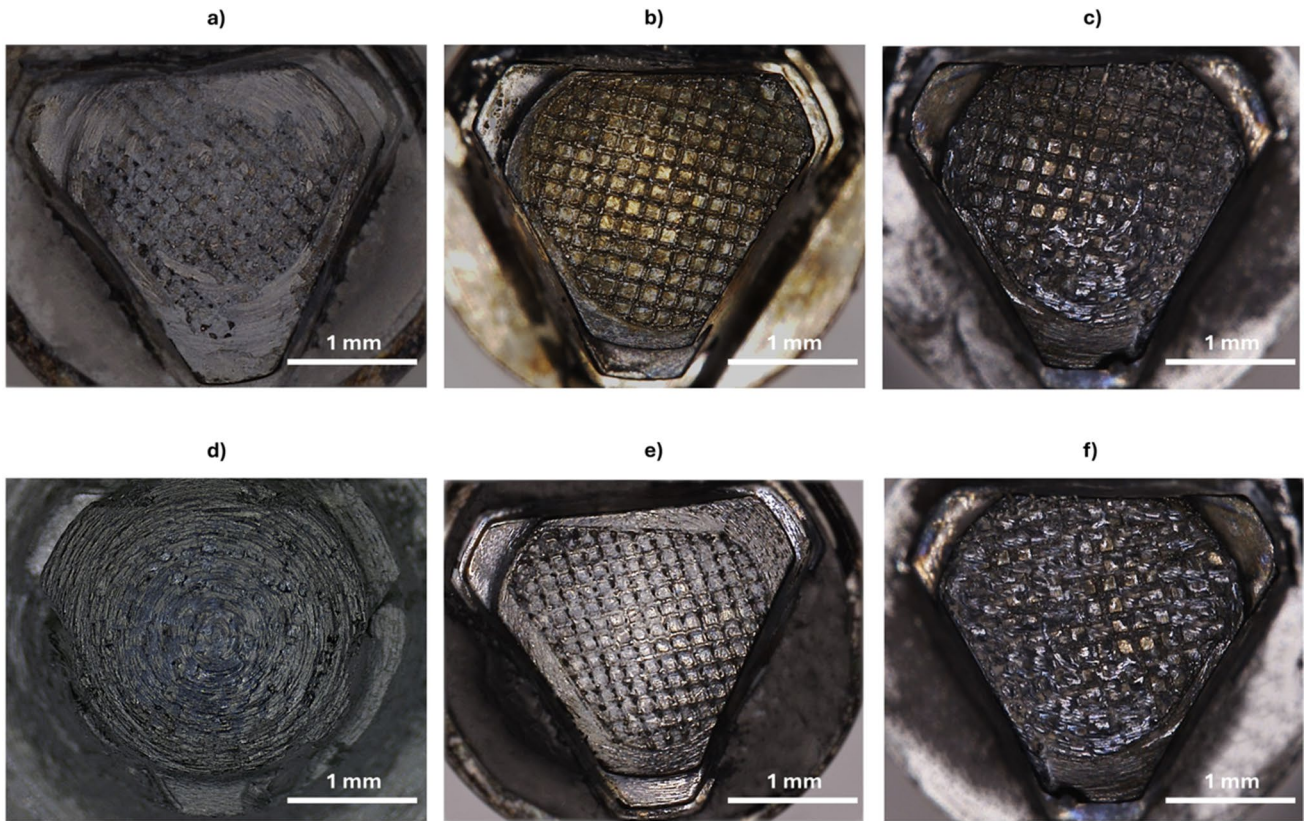
Fig. 6 Pin comparison in the examined conditions: **a**) Used Tool, **b**) More Used Tool, **c**) Cleaned-Used Tool, **d**) Cleaned-More Used Tool, **e**) Increased Speed-Used Tool, **f**) Increased Speed-More Used Tool
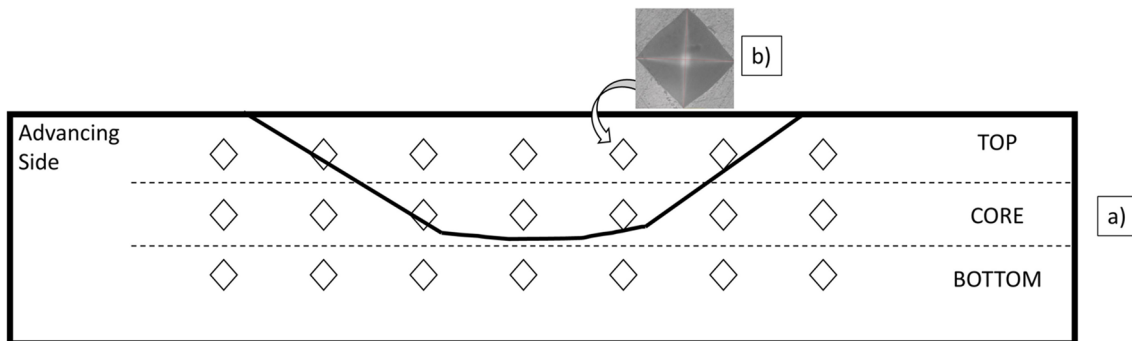

Fig. 7 **a**) Schematic representation of the indentations grid performed on each specimen, **b**) SEM image of a microhardness indentation

treated, some peaks can be seen (highlighted by arrows in the picture) and can be attributed to different plunging stages (peak A: plunging of the tip of the pin; peak B: plunging of the shoulder; peak C: further plunging of the shoulder to reach the desired plunging depth); II) dwelling phase: the tool is plunged within the plate but is not travelling, the purpose of this stage is to soften the material before the processing starts, the power appears quite constant with a slight decrease due to the softening of the material; III) processing or travel phase: the tool starts to travel the processing path at the desired travel speed, the power required suddenly peaks, and then achieves a kind of steady state value, some peaks are still present and can be attributed to the complex phenomena occurring during the process.

As a first result, it can be noted that the power consumption diagram well describes the phenomena occurring during the process and all the different phases of the process can be clearly evidenced from the diagram. An interesting consideration can be made by looking at the plot relative to the MUT sample (see Table 2), shown in Fig. 10.

**Fig. 8** Picture of the top view of all the treated tracks
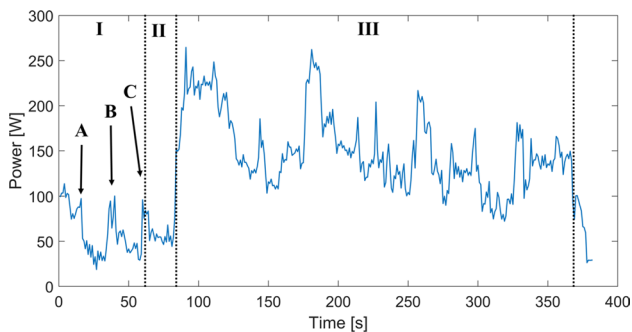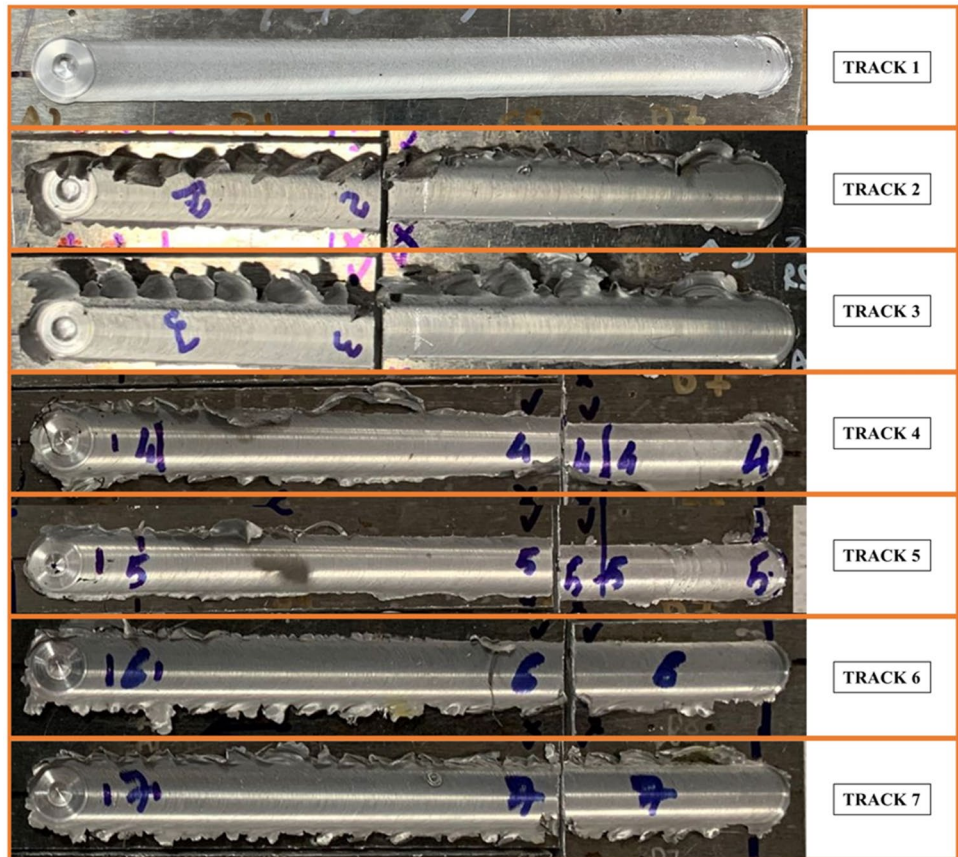
Fig. 9 Power consumption versus time for the NT sample
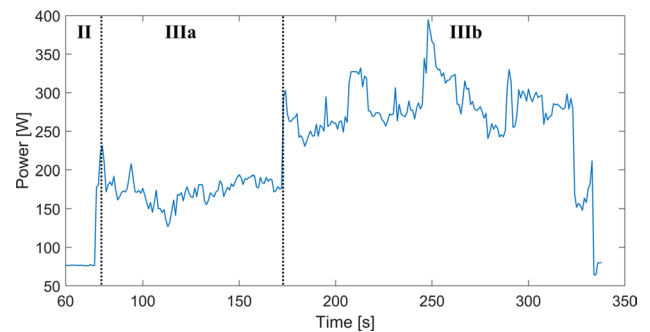
Fig. 10 Power consumption versus time for the MUT sample

The diagram depicted in Fig. 10 starts from the previously described phase II and focuses on the processing phase, namely phase III. In this case, two distinct sub-phases can be identified within phase III: phase IIIa and phase IIIb. In particular, a significant power peak is observed during the processing, after which the measured power remains at high values. This peak acts as a demarcation point between the two sub-phases. It is important to recall that this experiment was conducted using a highly worn tool, i.e. MUT condition, and the observed increase in power suggests an event occurred within the tool that

led to the peak and subsequent rise in power consumption. This phenomenon is similar to what happens in machining when a BUE is formed. After the failure of BUE, a power peak is experienced, followed by a higher steady-state power consumption [53]. So, it can be argued that a wear-related phenomenon occurs and determines the peak and the increase of power consumption. Another interesting observation is that also in phase IIIa, the average power consumption is higher than the one observed in NT sample during phase III. This result suggests that a phenomenon associated with tool usage is present, resulting in
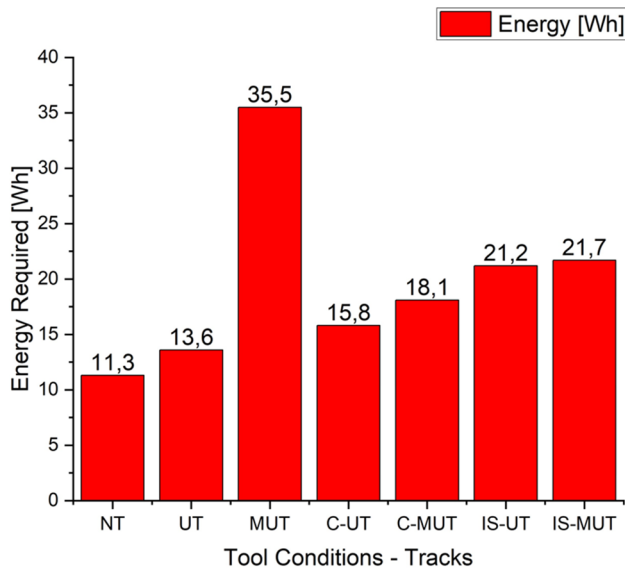
Fig. 11 Energy required to perform the different FSP tracks with different tool conditions

Fig. 12 Comparison of temperature measurements for IS-UT sample

an increased power requirement. At a certain point, these use-related phenomena turn into wear-related phenomena.

Elaborating the power acquisitions, it is possible to calculate the energy required for each FSP track. The results are presented in the diagram shown in Fig. 11, where the energy required to perform each track is plotted.

Looking at the diagram, some considerations can be clearly highlighted. The first consideration concerns the first three samples, where the tool conditions were labeled as "New", "Used", and "More Used": when the tool was new (NT sample), the minimum value of required energy was observed, this value increased with increasing tool service, reaching the maximum value in the FSP process with the MUT sample (the energy required is three times higher than the initial one). The second consideration refers to C-UT and C-MUT samples: the cleaning step had a positive effect on reducing energy consumption. Although the energy requirement remains slightly higher compared to that of a new tool, it is remarkably close to it. The third consideration refers to the IS-UT and IS-MUT samples: increasing the TRS also reduced the required energy with respect to the MUT sample. Although the energy values are slightly higher in these cases than those achieved through tool cleaning, this strategy eliminates the need for tool pause or replacement, resulting in time-saving by reducing machine idle time.

In addition to the energy analysis, the examination of temperature measurements provides valuable insights. Due to the complexity of the phenomena and the extensive amount of data recorded, a careful selection process was made to choose the diagrams to be presented and discussed in this section. It is important to note that, out of the eight
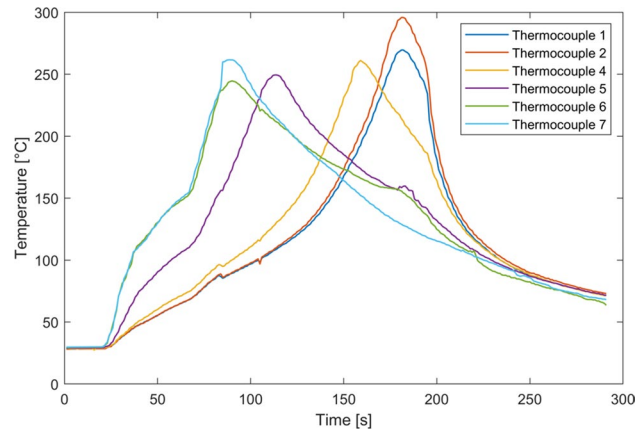
thermocouples mounted on the sheets for each FSP track (see Fig. 3), only the measurements from the six thermocouples closest to the given track were considered. Figure 12 and Fig. 13 display the temperature measurements specifically for IS-UT (see Table 2), although all tracks exhibited similar behavior with variations in peak values. Therefore, the discussion of the curves in Fig. 12 and Fig. 13 is applicable to all the performed experiments.

It is possible to observe that all the curves showed the same behavior: at the beginning, the temperature measured by each thermocouple is at room temperature; as the tool approached the thermocouple, the temperature gradually increased, reaching its maximum value when the tool crossed the thermocouple; subsequently, the temperature started to decrease. All the thermocouples showed similar peak values, proving the reliability and consistency of the process. The thermocouples positioned at the end of the processed path showed a slight increase in the maximum measured temperature, that can be attributed to the continuous heating up experienced by the plate during the process. It is also worth recalling that the values recorded by the thermocouples were proportional to the temperature achieved in the processed area but represent, of course, only a fraction of the actual temperature. Given the aim of this work, i.e., comparing the results of different tracks, this approximation can be accepted as long as the distance where the thermocouples are placed is constant for all the FSP tracks.

In Fig. 14 is reported a histogram showing the maximum values recorded for each FSP track. These values were calculated as the mean of the maximum temperature measured by each of the six thermocouples considered for each respective track.

Looking at the diagram, two considerations can be highlighted: i) the temperature increased with the TRS; ii) the temperature decreased with the increase of the tool usage. While the former is an expected outcome, as higher TRS
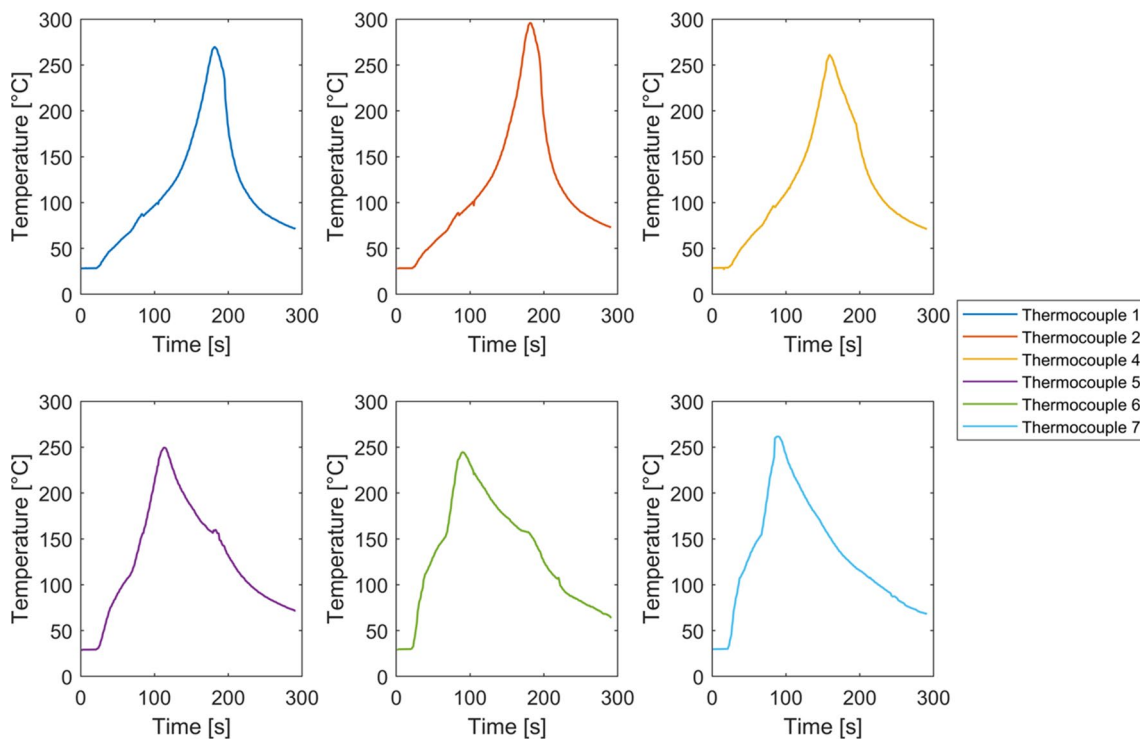
Fig. 13 Temperature measurements for IS-UT sample of each thermocouple
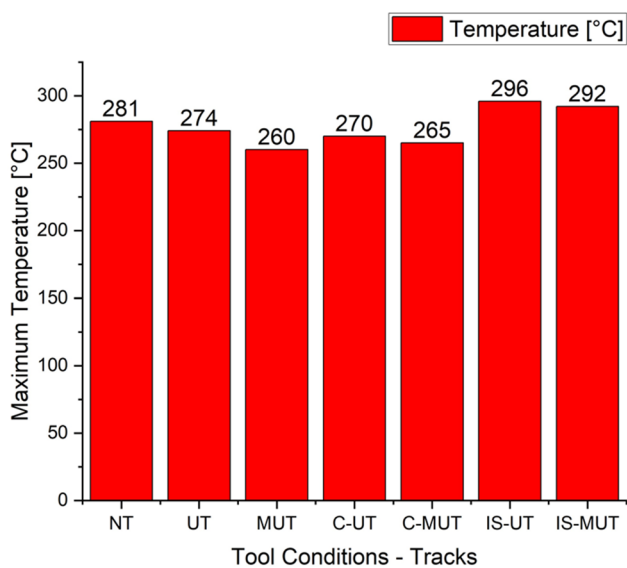

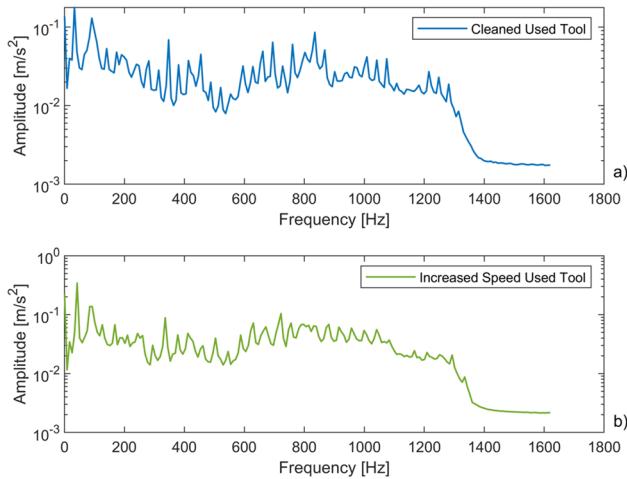**Fig. 14** Maximum temperature measured for each track

results in increased heat input [17], the latter deserves a more detailed explanation. In friction stir processes, heat generation is due to two mechanisms: the friction between the tool's shoulder and the top surfaces of the plates, and the friction between the tool's pin and the stirred material, it is generally agreed that most of the heat is generated by the tool [17, 54]. Based on these comments and the observed

results, it can be argued that adhesive wear occurring on the tool during the process (characterized by the accumulation of processed material on the tool's surface, creating a kind of BUE) reduces the efficiency of the friction action, resulting in a reduction in the temperatures reached during the process. This reduction of heat generation also accounts for the observed increase in the required power: aluminum's mechanical properties are strictly related to the temperature [55–57], and a lower temperature involves a reduced softening of the material, leading to a higher power required to stir and mix the material.
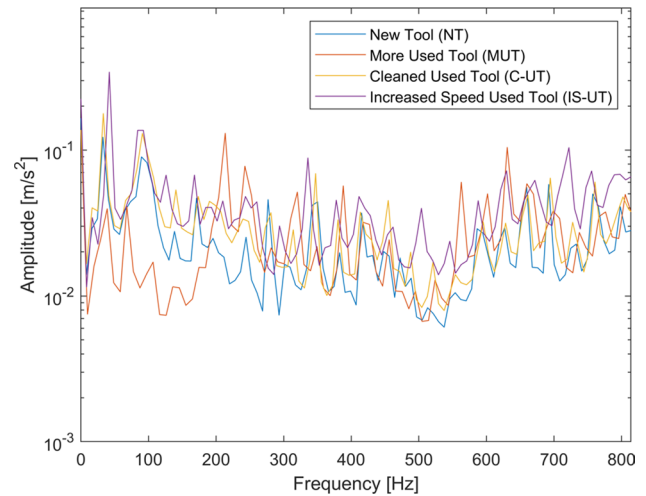
As a further analysis, the vibrations during the FSP process were acquired by means of the PulseNG accelerometer with the aim to evaluate the effects in the seven different conditions (Table 2). The data were collected for a time of about 400 s for each test and the accelerometer sampling rate was set to 3241 Hz. In particular, the acceleration data were analyzed in the transformed domain, i.e., the accelerometer signal spectrum was obtained by means of the Fast Fourier Transform (FFT). The tests were conducted with two different TRSs i.e. 2000 rpm and 2500 rpm, to which correspond frequencies of 33.3 Hz and 41.7 Hz, respectively. So, the analyses conducted on frequency are evaluated in the observation window following the effect of rotational speed. As shown in Fig. 15a, the results highlight that in the NT sample, the maximum amplitude value was 0.12 m/s^2
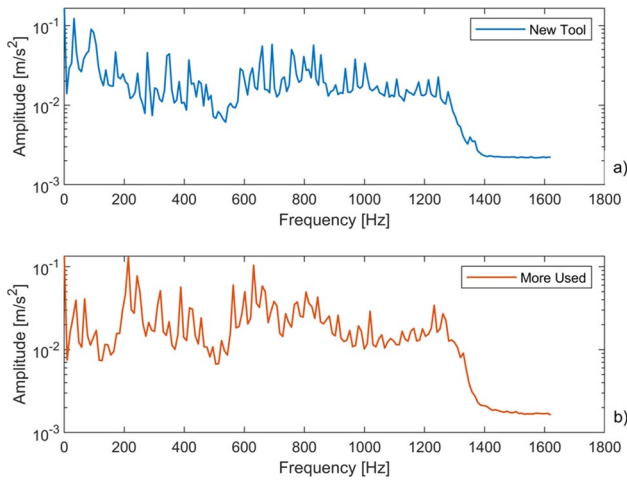
Fig. 15 One-side accelerometer signal spectrum: **a)** NT sample, **b)** MUT sample

Fig. 16 One-side accelerometer signal spectrum: **a)** C-UT, **b)** IS-UT

Fig. 17 Comparison of Accelerometer Spectrum in test cases

Table 3 Vibration amplitude and frequency results in the observation window

Sample	Code	Amplitude $[m/s^2]$	Vibration Frequency [Hz]
1	NT	0.09	89.5
2	UT	0.13	209.7
3	MUT	0.13	213.5
4	C-UT	0.13	90.9
5	C-MUT	0.09	89.5
6	IS-UT	0.13	83.9
7	IS-MUT	0.12	91.8

at 32 Hz, and the second maximum value was 0.09 m/s^2 at 89 Hz, while the MUT sample shows a peak value at 213 Hz with the same amplitude value (Fig. 15b). On the other hand, Fig. 16a shows the fourth case (C-UT sample), where the vibration frequency was equal to 33 Hz and the maximum amplitude value was 0.17 m/s^2 and second maximum value was 0.13 m/s^2 at 90 Hz, while Fig. 16b shows the results of IS-UT sample, that highlights the maximum amplitude value equal to 0.20 m/s^2 at 41 Hz and the second maximum amplitude value equal to 0.13 m/s^2 at 83 Hz. For the sake of clarity, only four tests are shown in Fig. 15 and Fig. 16, which are then compared in Fig. 17, while the maximum amplitude values at the corresponding frequency are reported in Table 3, according to the defined observation window i.e., subsequent to the rotation frequency.

Therefore, the results highlighted that as the pin wear increased, effects in terms of vibration were observed at frequencies on the order of about 200 Hz while increasing the TRS gave comparable results in terms of vibration effects to the cleaned tool. In addition, by considering the observation window following the rotation frequency, anomalies and, in the specific case, pin wear can be identified through the use of the FFT on the acceleration data.

The analysis of the Vickers microhardness also led to interesting observations. Figure 18 presents the microhardness measurements for the FSP track that exhibited the lowest temperatures (MUT sample) and the highest temperature (IS-UT sample).

The microhardness achieved in the friction stir processed area is the result of very complex phenomena, including the temperature reached during the process, the amount of plastic deformation, the experienced strain rate and the occurrence of dynamic recrystallization phenomena [17]. Therefore, inferring the exact influence of the tool condition and temperature achieved is quite complex,
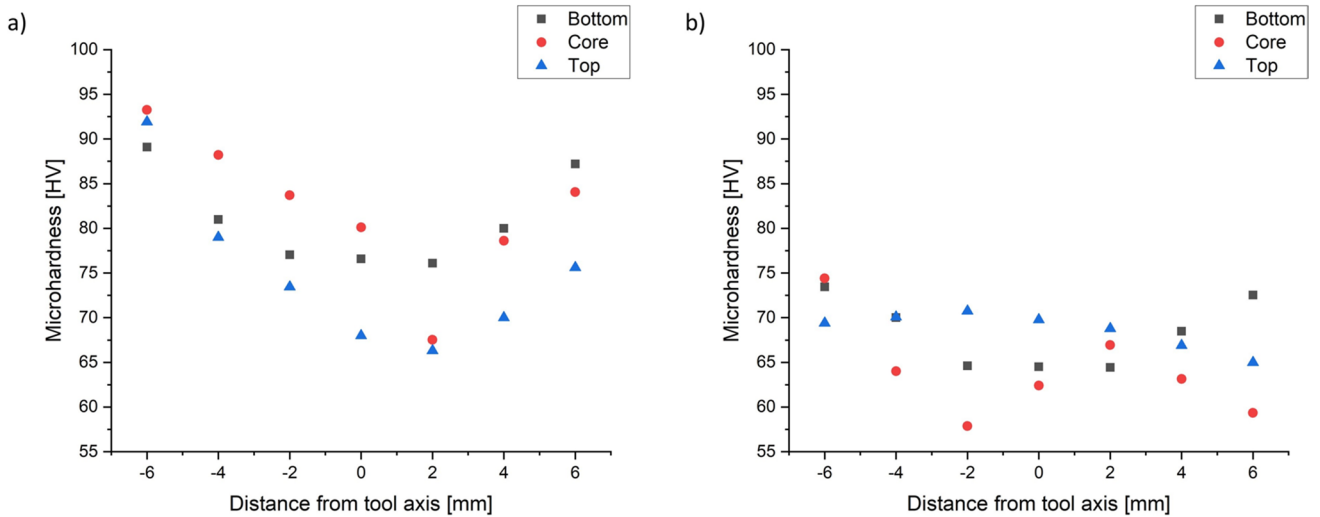
Fig. 18 Vickers microhardness measurements for **a**) MUT sample, and **b**) IS-UT sample

however, some considerations can still be drawn. Firstly, it is possible to observe that the microhardness increased as the temperature decreased, which is coherent with the available literature [58, 59]. Then, it can be noted that as the tool wear increased, the differences between the advancing side (AS) and retreating side (RS) become more pronounced, suggesting a more asymmetric and irregular material flow during the process.

The macrographic observations highlighted the absence of defects, as shown in Fig. 19.

Moreover, in all the samples it is possible to observe the refinement of the grains in the nugget zone in comparison with the base material (BM). A representative example is shown in Fig. 20, focusing on the IS-MUT sample. The figure illustrates the presence of the nugget zone (NZ), the thermomechanical affected zone (TMAZ) on both the advancing and retreating side, as well as the BM. The NZ is composed of equiaxial grains resulting from the dynamic recrystallization, induced by the stirring and deformation of the material at high temperatures and strain (Fig. 20a and b). In contrast, the TMAZ experiences comparatively lower
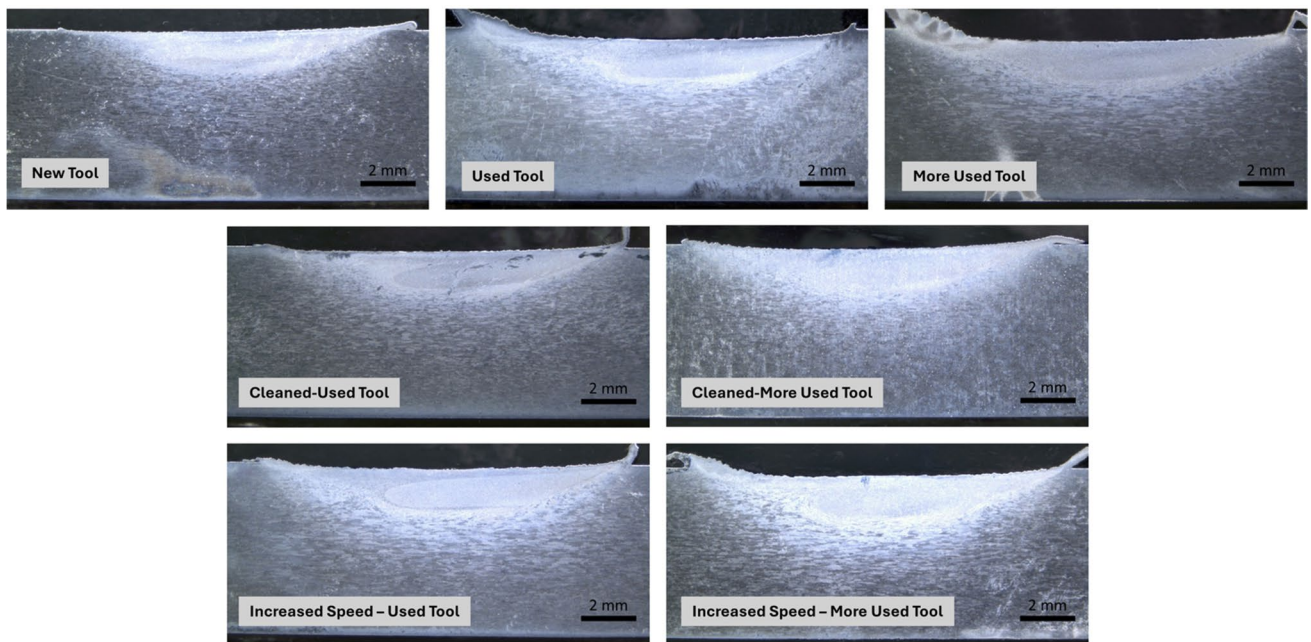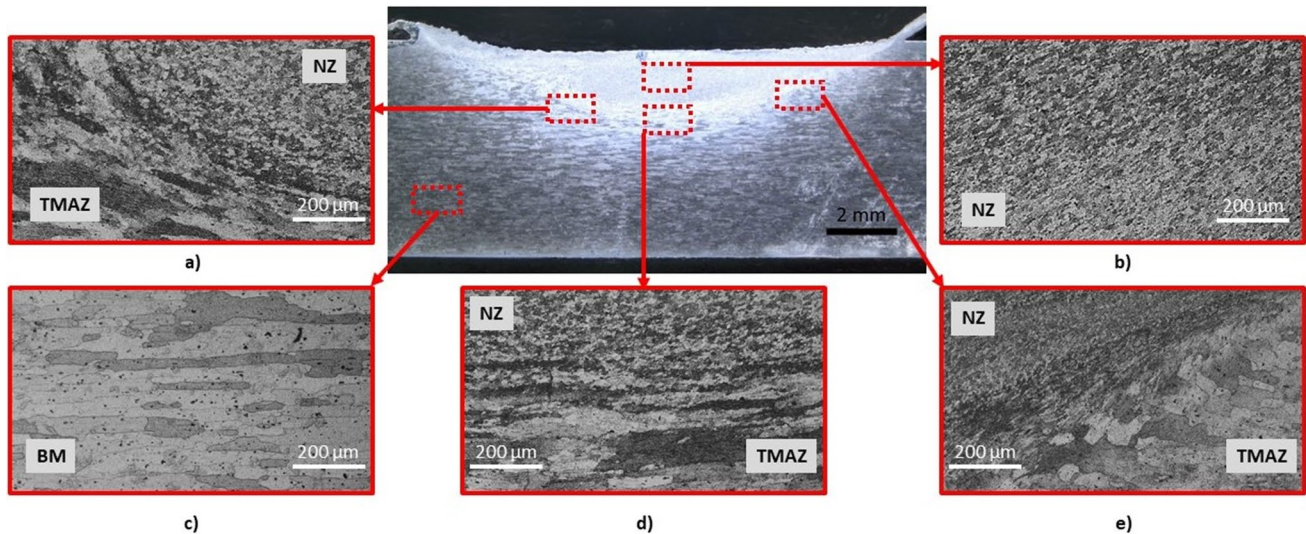

Fig. 19 Micrographics of all the performed tracks

Fig. 20 Microstructure of the different zones for the IS-MUT sample: **a**) Thermomechanical Affected Zone and Nugget Zone in the retreating side, **b**) Nugget, **c**) Base Material, **d**) Nugget Zone and Thermo- mechanical Affected Zone in the bottom side, **e**) Nugget Zone and Thermomechanical Affected Zone in the advancing side

heat input and less material stirring and movement compared to the NZ, resulting in stretched and deformed grains, but without undergoing full recrystallization (Fig. 20a, d and e).

An interesting consideration can be made in relation to the pin volume ratio, i.e. the dynamic volume to static volume ratio. As mentioned above, the role of the tool pin is to stir the material and move it behind to achieve a sound joint. The pin's geometry significantly influences material flow and consequently, the pin volume ratio is influenced by the pin's geometry [60–62]. Figure 21 illustrates the outcomes related to the pin volume ratio for each condition, and it is possible to note a distinct trend, showcasing that the stirring zone undergoes variations with tool wear. This variation indicates the alteration of the tool's initial shape, rendering it no longer applicable to label the tool as non-consumable. Notably, the pin volume ratio decreases from the new tool condition to the more used state. After the cleaning phase, this value increases, albeit not fully regaining the initial value. Subsequently, there is a further decrement observed in the last two conditions, i.e. IS-UT and IS-MUT.

4 Discussion

4.1 Tool wear

In the literature, it is widely accepted that a steel tool used for welding or processing aluminum sheets can be considered non-consumable, and its wear can be neglected [44–46], this assessment is based on the observation indicating that the tool retains its initial shape after the process,
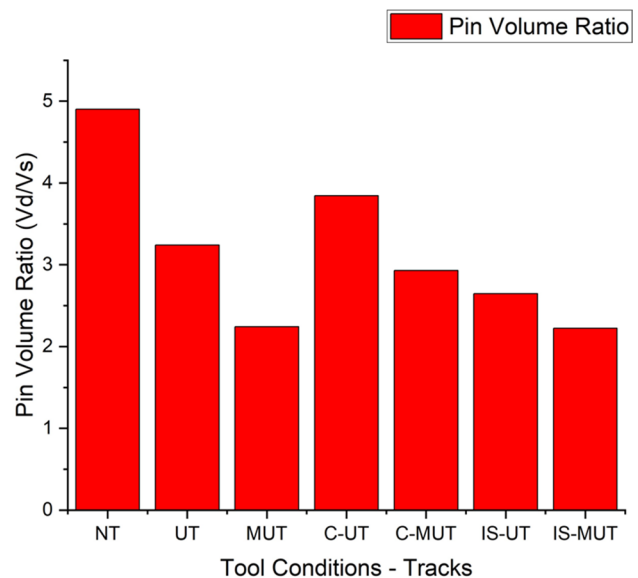
Fig. 21 Pin volume ratio versus tool conditions

and no abrasive wear can be observed. Instead, the adhesion of aluminum was observed, although easily removable to restore the tool to its initial shape. Moreover, it was noted that using a "used" tool did not impact the performance of the joints or treated parts. However, this assumption falls short in considering the energy consumption during the process and the overall behavior of the tool. As shown in previous section, it is possible to see that the energy required to perform a given process varies with the tool conditions. The motivation of this outcome can be explained by introducing

the following mechanism. During the process, there are two main factors to be considered: i) the interaction between the tool shoulder and the top surface of the sheets; ii) the interaction between the tool pin and the stirred material. It can be also introduced that, during the process, due to the high temperatures and the high contact pressures, adhesion phenomena occur between the processed aluminum and the steel tool, in particular, some adhered aluminum can be found on both the shoulder and the pin, as shown in Fig. 22. This phenomenon can be considered, under some aspects, similar to the built-up edge observed on the rake face of cutting tools [63]. The formation of this kind of BUE affects the contact condition between the tool and the material resulting in an altered material flow.

The adhesion of material on the shoulder changes the contact conditions between the shoulder and the sheets. Considering that the shoulder exerts a forging action, confining the material in the processed zone and preventing excessive flash formation [45], it can be argued that the adhered aluminum influences the role played by the shoulder: in fact, it is possible to observe a more pronounced flash when the tool became more used (refer to Fig. 8), suggesting that this adhered material limits the effectiveness of the shoulder in confining the processed material. Regarding the tool's pin, the adhered material affects its stirring action leading to a more complex material flow. As a result, a more asymmetric hardness distribution between the advancing side and retreating side can be observed. Moreover, both the shoulder and the pin contribute to the generation of the frictional heat required to soften the material. Considering that the temperature decreases with the increase of the tool service life, it is possible to assess that this adhesion phenomenon also leads to less efficient heat generation. The lower heat generated, and the consequent lower temperatures achieved lead to a lesser softening of the material, resulting in higher forces required to stir the material and higher energy consumption to perform the process.

Summarizing, it can be concluded that the tool experiences adhesive wear, leading to the formation of a kind of BUE that could be called BUTI (Built-Up Tool Interface), which changes the material flow (altering the flash formation and the microhardness distribution) and reduces the effectiveness of the heat generation mechanism (leading to higher power required to perform the process and so to higher energy consumption). On this basis, it could be possible to define a tool life beyond which the process became too energy-consuming. The definition of such duration would be of great interest for industrial applications where large amounts of material need to be processed.

4.2 Energy Consumption

In FSP, the main forces involved are the vertical force (required to keep the tool plunged within the material, whose application direction can be considered coaxial with the rotating tool) and the force opposing to the tool's travel (acting in-plane force on a plate's plane to be treated, with the same application direction of the tool's advancing speed) [64]. Additionally, the torque necessary to stir the material and keep the tool rotating should be considered. An important factor is the temperature achieved during the process: the higher the temperature, the greater the softening of the material, resulting in lower forces required to process the material. The overall energy consumption during the process can be divided into three components: i) the energy required to keep the machine running; ii) the energy related to the spindle rotation and workpiece table travel; iii) the energy needed to process the material. The first component depends mainly on the machine and its auxiliary units and so can be considered constant, while the second and third components are strongly influenced by the process parameters and material properties. As previously shown, the adhesive wear experienced by the tool leads
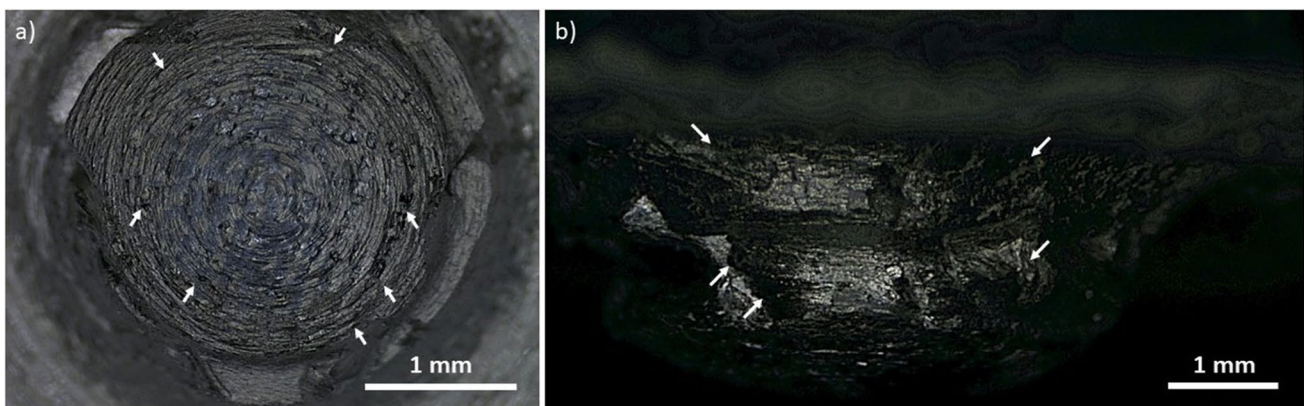

Fig. 22 More Used Tool: **a**) top view and **b**) side view

to lower temperatures achieved, resulting in less softening of the material; this, in turn, requires higher power to process the material and leads to higher energy consumption. It can be noted that the energy consumption increased with the tool wear, leading to two main considerations: i) monitoring the power can also help in monitoring the tool conditions, as done in machining [59, 65]; ii) it can be defined a tool service life beyond which the process became too energy consuming, and a maintenance action on the tool could be considered.

4.3 Tool Maintenance

Aiming to introduce a strategy to mitigate the increment of energy consumption due to the tool wear, two different strategies were investigated: i) cleaning the tool with a sodium hydroxide solution; ii) increasing the TRS to compensate for the reduction in heat generation. The approaches behind these two methodologies are completely different. In the first case, the proposed method involves stopping the process and cleaning the tool to remove as much adhered material as possible. In the second case, an increase in TRS is proposed to enhance contact velocity and promote the dissipation of more energy. The first solution involves a stop of the process, while the second involves an increase of the previously mentioned second component of energy consumption. The results showed that when the tool was cleaned, a noticeable reduction in the required energy is observed compared to the worn tool (C-UT and C-MUT vs MUT). However, the energy was still higher than that required for the case of a new tool, probably because the cleaning process is unable to remove all the adhered material. The cleaning process requires a stop and introduces a new working step, i.e., tool cleaning, so its application in an industrial environment should be carefully considered.

The second proposed method, i.e., the increase of TRS, also reduced the required energy with respect to the worn tool but required higher energy than the cleaned tool. In this case, two aspects need to be considered. On one hand, the increase of TRS requires higher energy to bring the spindle to this higher velocity, on the other hand, the increased temperature (see Fig. 14), leads to increased softening of the material, resulting in a reduction of the torque required to stir the material. The interaction between these two phenomena leads to a positive balance, resulting in the observed reduction of the required energy. This strategy does not require a process stop but cannot be endlessly repeated by continuously increasing the TRS, considering that it is limited by the maximum temperatures compatible with a sound and well-performing process and the maximum spindle speed available.

4.4 Sustainability of the Process

Usually, in FSP, the choice of the process parameters is only driven by the performances of the treated parts [2, 66], for example, a process window is suggested based on the good properties of the final part. However, it is important to consider the sustainability of the process as a parameter to support decision-making. Within the processing window, where different combinations of process parameters can lead to good properties of the final part, the combinations that result in lower energy consumption should be chosen. Additionally, an adequate maintenance strategy should be implemented for long-lasting processes. In selecting the process parameters, the balance between the energy required to accelerate the spindle and the softening reached by the material should be considered. Monitoring the tool condition should also be taken into account to adjust the process parameters according to the tool conditions (to promote material softening) or to plan a maintenance strategy for the tool.

5 Conclusions

In this study, a method to monitor the tool condition is proposed by investigating its influence on the FSP of aluminum sheets and its impact on energy consumption. Based on the outcomes, the following conclusions can be drawn:

– The tool can no longer considered "non-consumable" on the basis of the observed adhesive wear, indeed the energy requirements, the achieved temperatures and vibrations during the FSP process, vary depending on the tool condition. The measurements of energy consumption, temperature and vibrations have proven to be useful methods for monitoring tool conditions.
– Adhesive wear on the tool was observed, leading to the formation of a built-up tool interface (BUTI) caused by the adhesion of aluminum material. The BUTI altered the material flow dynamics and reduced the efficiency of heat generation, resulting in increased power requirements to stir the material. Consequently, the tool can be considered "worn" or "consumed" when the power required for the process exceeds a certain threshold. Based on these findings, it becomes possible to establish a tool lifespan, after which the process becomes excessively energy-consuming. Determining such a duration is of significant value for industrial applications that requires extensive material processing.
– Two strategies were proposed to mitigate the increment in energy consumption associated with the tool condition: cleaning the tool with a sodium hydroxide solution and increasing the tool's rotational speed

to compensate for the reduction in heat generation. These strategies have a positive impact on reducing energy consumption. Although the energy requirement remains slightly higher than that of a new tool, it is remarkably close. This highlights the effectiveness of cleaning in restoring the tool's performance and reducing energy consumption. On the other hand, increasing tool rotational speed prevents the process from stopping but cannot be endlessly repeated.

– The outcomes highlight that by serving a process monitoring method, such as measurements of energy consumptions, temperatures and vibrations, a more sustainable selection of process parameters can be made. Within an identified processing window, where several combinations of parameters can lead to desirable part properties, preference should be given to combinations that minimize energy consumption, additionally implementing an appropriate maintenance strategy for the tool.

In conclusion, the present work proposed methods for monitoring the tool during the service under various conditions measuring the energy requirements, temperatures and vibrations. The impact of tool wear on power requirements was analyzed, and it was expanded the understanding of tool behavior and its implications for the overall process performance. By prioritizing energy efficiency and implementing effective maintenance strategies, the sustainability of the FSP process can be enhanced, making it a viable option for industrial applications requiring large-scale material processing.

Nomenclature AA: Aluminum Alloy; BM: Base Material; BUE: Build-Up Edge; BUTI: Built-Up Tool Interface; C-UT: Cleaned-Used Tool; C-MUT: Cleaned-More Used Tool; FSP: Friction Stir Processing; FSW: Friction Stir Welding; IS-UT: Increased rotational Speed-Used Tool; IS-MUT: Increased rotational Speed-More Used Tool; MEMS: Micro-Electromechanical Sensors; MUT: More Used Tool; NT: New Tool; NZ: Nugget Zone; TMAZ: Thermo-Mechanical Affected Zone; TRS: Tool Rotational Speed; UT: Used Tool

Data Availability Data sharing is not applicable to this article.

Declarations

Conflict of Interest The authors declare no conflict of interest.

References

1. Rathinasuriyan, C., Pavithra, E., Sankar, R., & Senthil Kumar, V. S. (2021). Current Status and Development of Submerged Friction Stir Welding: A Review. *International Journal of Precision Engineering and Manufacturing - Green Technology*. https://doi.org/10.1007/s40684-020-00187-6

2. Jain, R., Kumari, K., Kesharwani, R. K., Kumar, S., Pal, S. K., Singh, S. B., Panda, S. K., & Samantaray, A. K. (2015). Friction stir welding: Scope and recent development. In J. P. Davim (Ed.), *Modern manufacturing engineering* (pp. 179–229). https://doi.org/10.1007/978-3-319-20152-8_6

3. Wang, T., Upadhyay, P., & Whalen, S. (2021). A Review of Technologies for Welding Magnesium Alloys to Steels. *International Journal of Precision Engineering and Manufacturing - Green Technology*. https://doi.org/10.1007/s40684-020-00247-x

4. Cabibbo, M., Forcellese, A., Santecchia, E., Paoletti, C., Spigarelli, S., & Simoncini, M. (2020). New approaches to friction stir welding of aluminum light-alloys. *Metals*. https://doi.org/10.3390/met10020233

5. Hammood, A. S., Esmailzadeh, M., Hosseini, S. N., Karimi, S., Calliari, I., Pezzato, L., & Brittain, R. (2023). Effect of Friction Stir Welding Parameters on Microstructure and Corrosion Behavior of 2101 Duplex Stainless Steel in Simulated Body Fluid. *International Journal of Precision Engineering and Manufacturing - Green Technology, 10*, 327–337. https://doi.org/10.1007/s40684-022-00440-0

6. Laska, A., Szkodo, M., Pawłowski, Ł, & Gajowiec, G. (2023). Corrosion Properties of Dissimilar AA6082/AA6060 Friction Stir Welded Butt Joints in Different NaCl Concentrations. *International Journal of Precision Engineering and Manufacturing - Green Technology, 10*, 457–477. https://doi.org/10.1007/s40684-022-00441-z

7. Fratini, L., Buffa, G., & Shivpuri, R. (2009). In-process heat treatments to improve FS-welded butt joints. *International Journal of Advanced Manufacturing Technology, 43*, 664–670. https://doi.org/10.1007/s00170-008-1750-8

8. Aldanondo, E., Arruti, E., Alvarez, P., & Echeverria, A. (2016). Mechanical and microstructural properties of FSW lap joints. *Friction Stir Welding and Processing VII* (pp. 195–203). Springer International Publishing. https://doi.org/10.1007/978-3-319-48108-1_20

9. Shojaeefard, M. H., Akbari, M., & Asadi, P. (2014). Multi objective optimization of friction stir welding parameters using FEM and neural network. *International Journal of Precision Engineering and Manufacturing, 15*, 2351–2356. https://doi.org/10.1007/s12541-014-0600-x

10. Dwivedi, M., Silvestri, A. T., Franchitti, S., Krishnaswamy, H., Narayanaperumal, A., & Astarita, A. (2021). Friction welding: An effective joining process for hybrid additive manufacturing. *CIRP Journal of Manufacturing Science and Technology*. https://doi.org/10.1016/j.cirpj.2021.07.016

11. Quarto, M., Bocchi, S., D'Urso, G., & Giardini, C. (2022). Hybrid finite elements method-artificial neural network approach for hardness prediction of AA6082 friction stir welded joints. *International Journal of Mechatronics and Manufacturing Systems, 15*, 149–166. https://doi.org/10.1504/ijmms.2022.124919

12. Silvestri, A. T., Parodo, G., Napolitano, F., El Hassanin, A., Scherillo, F., Sorrentino, L., & Squillace, A. (2024). Cold formability of friction stir processed 5754–H111 and 6082–T6 aluminum alloys: An experimental and numerical study. *The International Journal of Advanced Manufacturing Technology*. https://doi.org/10.1007/s00170-024-13218-2

13. Mishra, R. S., Mahoney, M. W., McFadden, S. X., Mara, N. A., & Mukherjee, A. K. (1999). High strain rate superplasticity in a friction stir processed 7075 Al alloy. *Scripta Materialia, 42*, 163–168. https://doi.org/10.1016/S1359-6462(99)00329-2

14. Mishra, R. S., & Mahoney, M. W. (2001). Friction stir processing: A new grain refinement technique to achieve high strain rate superplasticity in commercial alloys. *In Materials Science Forum, 357–359*, 507–514. https://doi.org/10.4028/www.scientific.net/msf.357-359.507

15. Węglowski, M. S. (2018). Friction stir processing–State of the art. *Archives of Civil and Mechanical Engineering, 18*(1), 114–129. https://doi.org/10.1016/j.acme.2017.06.002

16. Jadav, H. H., Badheka, V., Sharma, D. K., & Upadhyay, G. (2020). A review on effect of friction stir processing on the welded joints. *Materials Today: Proceedings, 43*, 84–92. https://doi.org/10.1016/j.matpr.2020.11.215

17. Mishra, R. S., & Ma, Z. Y. (2005). Friction stir welding and processing. *Materials science and engineering: R: reports, 50*, 1–78. https://doi.org/10.1016/j.mser.2005.07.001

18. Zhou, H., Kong, X., Luo, J., An, Q., & Li, H. (2023). Quality-Related Process Monitoring Based on a Bayesian Classifier. *International Journal of Precision Engineering and Manufacturing, 24*, 2197–2209. https://doi.org/10.1007/s12541-023-00896-3

19 Zhou, F., Fu, X., Chen, S., Kim, E., & Jun, M. B. G. (2023). Fiber Optic Sensor for Smart Manufacturing. *International Journal of Precision Engineering and Manufacturing-Smart Technology, 1*, 125–136.

20. Kim, S. W., Kong, J. H., Lee, S. W., & Lee, S. (2022). Recent Advances of Artificial Intelligence in Manufacturing Industrial Sectors: A Review. *International Journal of Precision Engineering and Manufacturing*. https://doi.org/10.1007/s12541-021-00600-3

21. Zhao, X., Li, C., Chen, X., Cui, J., & Cao, B. (2022). Data-driven cutting parameters optimization method in multiple configurations machining process for energy consumption and production time saving. *International Journal of Precision Engineering and Manufacturing - Green Technology, 9*, 709–728. https://doi.org/10.1007/s40684-021-00373-0

22. Lee, J., Chua, P. C., Chen, L., Ng, P. H. N., Kim, Y., Qiong, W., Jeon, S., Jung, J., Chang, S., & Moon, S. K. (2023). Key Enabling Technologies for Smart Factory in Automotive Industry: Status and Applications. *International Journal of Precision Engineering and Manufacturing-Smart Technology, 1*, 93–105. https://doi.org/10.57062/ijpem-st.2022.0017

23. Zuo, L., Shao, W., Zhang, X., & Zuo, D. (2022). Investigation on tool wear in friction stir welding of SiCp/Al composites. *Wear, 498*, 204331. https://doi.org/10.1016/j.wear.2022.204331

24. Tseng, H. C., Tsai, M. S., Yeh, B. C., & Li, K. M. (2022). Analysis of Tool Wear by Using a Cutting Bending Moment Model for Milling Processes. *International Journal of Precision Engineering and Manufacturing*. https://doi.org/10.1007/s12541-022-00680-9

25. Nam, J. S., & Kwon, W. T. (2022). A Study on Tool Breakage Detection During Milling Process Using LSTM-Autoencoder and Gaussian Mixture Model. *International Journal of Precision Engineering and Manufacturing, 23*, 667–675. https://doi.org/10.1007/s12541-022-00647-w

26. Li, B., Tian, X., & Zhang, M. (2022). Modeling and multi-objective optimization method of machine tool energy consumption considering tool wear. *International Journal of Precision Engineering and Manufacturing - Green Technology, 9*, 127–141. https://doi.org/10.1007/s40684-021-00320-z

27. Sahlot, P., & Arora, A. (2018). Numerical model for prediction of tool wear and worn-out pin profile during friction stir welding. *Wear, 408*, 96–107. https://doi.org/10.1016/j.wear.2018.05.007

28. Sahlot, P., Jha, K., Dey, G. K., & Amit, A. (2017). Quantitative wear analysis of H13 steel tool during friction stir welding of Cu-0.8%Cr-0.1%Zr alloy. *Wear, 378*, 82–89. https://doi.org/10.1016/j.wear.2017.02.009

29. Hasan, A. F., Bennett, C. J., Shipway, P. H., Cater, S., & Martin, J. (2017). A numerical methodology for predicting tool wear in Friction Stir Welding. *Journal of Materials Processing Technology, 241*, 129–140. https://doi.org/10.1016/j.jmatprotec.2016.11.009

30. Zhou, L., Mingrun, Y., Zhao, H., Jiang, Z., Guo, F., & Song, X. (2019). Dissimilar friction stir welding of AA6061 and Ti6Al4V alloys: A study on microstructure and mechanical properties. *Journal of Manufacturing Processes, 48*, 119–126. https://doi.org/10.1016/j.jmapro.2019.09.043

31. VenkatRamana, G., Yelamasetti, B., & Vishnu Vardhan, T. (2021). Effect of FSW process parameters and tool profile on mechanical properties of AA 5082 and AA 6061 welds. *Materials Today: Proceedings., 46*, 826–830. https://doi.org/10.1016/j.matpr.2020.12.801

32. Thompson, B., & Babu, S. S. (2010, December). Tool degradation characterization in the friction stir welding of hard metals. *Welding Journal.*. Retrieved June 15, 2023, from http://files.aws.org/wj/supplement/WJ122010_256.pdf

33. Gao, Z., Chen, M., Guo, W. G., & Li, J. (2020). Tool Wear Characterization and Monitoring with Hierarchical Spatio-Temporal Models for Micro-Friction Stir Welding. *Journal of Manufacturing Processes, 56*, 1353–1365. https://doi.org/10.1016/j.jmapro.2020.04.031

34. Das, H., Mondal, M., Hong, S. T., Chun, D. M., & Han, H. N. (2018). Joining and fabrication of metal matrix composites by friction stir welding/processing. *International Journal of Precision Engineering and Manufacturing - Green Technology, 5*, 151–172. https://doi.org/10.1007/s40684-018-0016-7

35. Weinberger, T., Khosa, S., Führer, B., & Enzinger, N. (2008). Analysis of tool wear and failure mechanism during friction stir welding of steel. In *7th international symposium on friction stir welding*.

36. Rai, R., De, A., Bhadeshia, H. K. D. H., & DebRoy, T. (2011). Review: Friction stir welding tools. *Science and Technology of Welding and Joining, 16*, 325–342. https://doi.org/10.1179/1362171811Y.0000000023

37. Pfeifer, T., & Wiegers, L. (2000). Reliable tool wear monitoring by optimized image and illumination control in machine vision. *Measurement Journal of the International Measurement Confederation, 28*, 209–218. https://doi.org/10.1016/S0263-2241(00)00014-2

38. Haber, R. E., Jiménez, J. E., Ronei Peres, C., & Alique, J. R. (2004). An investigation of tool-wear monitoring in a high-speed machining process. *Sensors and Actuators, A: Physical, 116*, 539–545. https://doi.org/10.1016/j.sna.2004.05.017

39. Shao, C., Kim, T. H., Jack Hu, S., Jin, J., Abell, J. A., & Patrick Spicer, J. (2016). Tool Wear Monitoring for Ultrasonic Metal Welding of Lithium-Ion Batteries. *Journal of Manufacturing Science and Engineering, Transactions of the ASME, 138*, 051005. https://doi.org/10.1115/1.4031677

40. Balachandar, K., Jegadeeshwaran, R., & Gandhikumar, D. (2019). Condition monitoring of FSW tool using vibration analysis-A machine learning approach. *Materials Today: Proceedings, 27*, 2970–2974. https://doi.org/10.1016/j.matpr.2020.04.903

41. Wang, G. F., Yang, Y. W., Zhang, Y. C., & Xie, Q. L. (2014). Vibration sensor based tool condition monitoring using ν support vector machine and locality preserving projection. *Sensors and Actuators, A: Physical, 209*, 24–32. https://doi.org/10.1016/j.sna.2014.01.004

42. Al-Badour, F., Mahgoub A., Bazoune, A., Shuaib, A., & Merah, N. (2017). On-line condition monitoring of friction stir spot welding tool using vibration measurements. In American society of mechanical engineers, pressure vessels and piping division (Publication) PVP (Vol. 6A-2017, PVP2017-65940). https://doi.org/10.1115/PVP2017-65940.

43. Rabi, J., Balusamy, T., & Raj Jawahar, R. (2019). Analysis of vibration signal responses on pre induced tunnel defects in friction stir welding using wavelet transform and empirical mode decomposition. *Defence Technology, 15*, 885–896. https://doi.org/10.1016/j.dt.2019.05.014

44. Prado, R. A., Murr, L. E., Shindo, D. J., & Soto, K. F. (2001). Tool wear in the friction-stir welding of aluminum alloy 6061 + 20% Al2O3: A preliminary study. *Scripta Materialia, 45*, 75–80. https://doi.org/10.1016/S1359-6462(01)00994-0

45. Ambrosio, D., Morisada, Y., Ushioda, K., & Fujii, H. (2023). Material flow in friction stir welding: A review. *Journal of Materials Processing Technology, 320*(118116). https://doi.org/10.1016/j.jmatprotec.2023.118116

46. Harikrishna, R., Patel, V., Buffa, G., Fratini, L., & Di Lorenzo, R. (2023). Influence of distinct tool pin geometries on aluminum 8090 FSW joint properties. In *Materials research proceedings* (Vol. 25, pp. 195–202). https://doi.org/10.21741/9781644902417-25

47. Ibrahim, H. K., Khuder, A. W. H., & Muhammed, M. A. S. (2019). Effect of tool-pin geometry on microstructure and temperature distribution in friction stir spot welds of similar AA2024-T3 aluminum alloys. *International Journal of Mechanical and Mechatronics Engineering, 19*, 14–28. International Journals of Engineering and Sciences Publisher.

48. Zain-ul-abdein, M., Nélias, D., Jullien, J. F., & Deloison, D. (2010). Experimental investigation and finite element simulation of laser beam welding induced residual stresses and distortions in thin sheets of AA 6056–T4. *Materials Science and Engineering: A, 527*, 3025–3039. https://doi.org/10.1016/j.msea.2010.01.054

49. Zain-ul-abdein, M., Nélias, D., Jullien, J. F., & Wagan, A. I. (2010). Thermo-mechanical characterisation of AA 6056–T4 and estimation of its material properties using Genetic Algorithm. *Materials and Design, 31*, 4302–4311. https://doi.org/10.1016/j.matdes.2010.03.056

50 Cozzolino, E., & Astarita, A. (2023). Energy saving in milling of electron beam–melted Ti6Al4V parts: influence of process parameters. *International Journal of Advanced Manufacturing Technology, 127*, 179–194. https://doi.org/10.1007/s00170-023-11502-1. Springer Science and Business Media Deutschland GmbH.

51. Astarita, A., Tucci, F., Silvestri, A. T., Perrella, M., Boccarusso, L., & Carlone, P. (2021). Dissimilar friction stir lap welding of AA2198 and AA7075 sheets: Forces, microstructure and mechanical properties. *International Journal of Advanced Manufacturing Technology*. https://doi.org/10.1007/s00170-021-07816-7

52. Tucci, F., Carlone, P., Silvestri, A. T., Parmar, H., & Astarita, A. (2021). Dissimilar friction stir lap welding of AA2198-AA6082: Process analysis and joint characterization. *CIRP Journal of Manufacturing Science and Technology*. https://doi.org/10.1016/j.cirpj.2021.09.007

53. Warsi, S. S., Jaffery, S. H. I., Ahmad, R., Khan, M., Agha, M. H., & Ali, L. (2018). Development and analysis of energy consumption map for high-speed machining of Al 6061–T6 alloy. *International Journal of Advanced Manufacturing Technology, 96*, 91–102. https://doi.org/10.1007/s00170-018-1588-7

54. Zhang, Y. N., Cao, X., Larose, S., & Wanjara, P. (2012). Review of tools for friction stir welding and processing. *Canadian Metallurgical Quarterly*. https://doi.org/10.1179/1879139512Y.0000000015

55 Ledbetter, H. M. (1982). Temperature behaviour of Young's moduli of forty engineering alloys. *Cryogenics, 22*, 653–656. https://doi.org/10.1016/0011-2275(82)90072-8

56. Nègre, P., Steglich, D., Brocks, W., & Koçak, M. (2003). Numerical simulation of crack extension in aluminium welds. *Computational Materials Science, 28*, 723–731. https://doi.org/10.1016/j.commatsci.2003.08.026

57. Sharma, S. C. (2000). Effect of albite particles on the coefficient of thermal expansion behavior of the Al6061 alloy composites. *Metallurgical and Materials Transactions A: Physical Metallurgy and Materials Science, 31*, 773–780. https://doi.org/10.1007/s11661-000-0019-0

58. Peel, M., Steuwer, A., Preuss, M., & Withers, P. J. (2003). Microstructure, mechanical properties and residual stresses as a function of welding speed in aluminium AA5083 friction stir welds. *Acta Materialia, 51*, 4791–4801. https://doi.org/10.1016/S1359-6454(03)00319-7

59. Mishra, D., Roy, R. B., Dutta, S., Pal, S. K., & Chakravarty, D. (2018). A review on sensor based monitoring and control of friction stir welding process and a roadmap to Industry 4.0. *Journal of Manufacturing Processes, 36*, 373–397. https://doi.org/10.1016/j.jmapro.2018.10.016. Elsevier.

60. Elangovan, K., & Balasubramanian, V. (2007). Influences of pin profile and rotational speed of the tool on the formation of friction stir processing zone in AA2219 aluminium alloy. *Materials Science and Engineering A, 459*, 7–18. https://doi.org/10.1016/j.msea.2006.12.124

61. Jain, R., Pal, S. K., & Singh, S. B. (2018). Finite element simulation of pin shape influence on material flow, forces in friction stir welding. *International Journal of Advanced Manufacturing Technology, 94*, 1781–1797. https://doi.org/10.1007/s00170-017-0215-3

62. Chandana, R., & Saraswathamma, K. (2023). Impact of tool pin profiles in friction stir welding process-A review. *Materials Today: Proceedings, 76*, 602–606. https://doi.org/10.1016/j.matpr.2022.12.097

63. Atlati, S., Haddag, B., Nouari, M., & Moufki, A. (2015). Effect of the local friction and contact nature on the Built-Up Edge formation process in machining ductile metals. *Tribology International, 90*, 217–227. https://doi.org/10.1016/j.triboint.2015.04.024

64. Astarita, A., Squillace, A., & Carrino, L. (2014). Experimental Study of the Forces Acting on the Tool in the Friction-Stir Welding of AA 2024 T3 Sheets. *Journal of Materials Engineering and Performance, 23*, 3754–3761. https://doi.org/10.1007/s11665-014-1140-3

65. Axinte, D., & Gindy, N. (2004). Assessment of the effectiveness of a spindle power signal for tool condition monitoring in machining processes. *International Journal of Production Research, 42*, 2679–2691. https://doi.org/10.1080/00207540410001671642

66. Colligan, K. J. (2010). Solid state joining: Fundamentals of friction stir welding. *Failure Mechanisms of Advanced Welding Processes*. https://doi.org/10.1533/9781845699765.137

Dr. Alessia Teresa Silvestri is a post-doctoral researcher at the University of Naples Federico II. She achieved cum laude the Master's Degree in Mechanical Engineering for Design and Production in 2018. She holds a Ph.D. in Technology, Innovation and Management from the University of Naples and the University of Bergamo in 2022. The doctoral studies focused on the optimization of process parameters in additive manufacturing technologies for tailored structures using different feedstock. Her scientific interests include solid state joining and additive manufacturing, both for metals (powder-bed-based, directed energy deposition) and polymers/composites (fused deposition modeling, continuous-fiber-fabrication).

Dr. Andrea El Hassanin is an Assistant Professor of the Department of Chemical Engineering, Materials and Industrial Production at the University of Naples Federico II. In 2016, He achieved cum laude the Master's Degree in Mechanical Engineering for Design and Production. Afterwards, in 2020 he achieved the Ph.D. in Products and Industrial Processes Engineering, presenting a thesis entitled "Post-process Surface Finishing Treatments for AlSi10Mg Parts made by Selective Laser Melting Technology". The main, but not the only, research activities of Dr. El Hassanin concern the study of additive manufacturing technologies, specifically considering parts made of metallic materials and their related surface treatments aimed at reducing surface roughness. At the same time, since the beginning of his career in 2016 to date, he has published a total of 36 articles, of which 22 in international scientific journals and 14 as papers of participation in international conferences. In parallel, Dr. El Hassanin has been involved in numerous consulting activities related to research projects carried out in the department.

Dr. Giorgio de Alteriis is an Assistant Professor in Mechanical and Thermal Measurements at the University of Naples Federico II. He has a Ph.D. in Technology, Innovation, and Management from the University of Naples Federico II and the University of Bergamo in 2022. He has a master's in Electronical Engineering from the University of Naples Federico II, cooperating with the Dept. of Industrial Engineering (DII) and Dept. of Electrical and Information Technology Engineering (DIETI). His doctoral studies focus on mechanical and thermal measurements and guidance navigation and control using MEMS technology for inertial navigation, measurements, and the data fusion algorithm. His research is currently oriented on innovative methods based on a redundant MEMS IMU configuration for bias and drift compensation. His scientific interests are also in microcontrollers and sensors for IoT-based distributed monitoring systems.

Prof. Antonello Astarita is associate professor in manufacturing at the University of Naples "Federico II", his research and teaching interests are related to the manufacturing processes of metals. He is co-author of more than 70 peer reviewed journal papers on these topics. Dr Astarita received the "ESAFORM Scientific Prize" in 2018 and the "ASM-IIM Lectureship Award" in 2016, he is in the editorial board of some journals with impact factor and is also member of the scientific committee of international conferences. He was visiting scientist at the University of Manchester and visiting professor at the University of Cadiz.